

## RESEARCH ARTICLE

View Article Online  
View Journal | View IssueCite this: *Org. Chem. Front.*, 2019, 6, 2839

## New synthetic approaches for hexacene and its application in thin-film transistors†

Jian Han,<sup>†a</sup> Xinbang Liu,<sup>†b</sup> Yu Li,<sup>c</sup> Zihao Lou,<sup>a</sup> Mingdong Yi,<sup>\*c</sup> Huihui Kong<sup>†b</sup> and Jun Luo<sup>†\*a</sup>

Hexacene is a valuable aromatic compound with special optoelectronic properties. Here, a stable new precursor of hexacene, 5,6,15,16-tetrahydro-5,16-epoxyhexacene, was synthesized through a three-step route in a total yield of 31%. Then two methods for the synthesis of hexacene based on this new precursor were developed. One is realized by dehydration of 5,6,15,16-tetrahydro-5,16-epoxyhexacene by thermal activation on the Cu(110) surface under ultrahigh vacuum (UHV) conditions. The other is copper powder-catalyzed dehydrogenation of another precursor 6,15-dihydrohexacene, which provided pure hexacene by vacuum sublimation in the dark. Organic thin-film transistors (OFETs) were fabricated using hexacene through a vacuum deposition method. And a comprehensive study of the hole-transfer properties of OFETs was performed. The best film mobility of hexacene was observed at  $0.123 \text{ cm}^2 \text{ V}^{-1} \text{ s}^{-1}$  with an on/off ratio of  $1.16 \times 10^4$  and a threshold of 2.65 V.

Received 31st May 2019,

Accepted 19th June 2019

DOI: 10.1039/c9qo00708c

rsc.li/frontiers-organic

## Introduction

Acenes are an important class of polycyclic aromatic hydrocarbons and have unique properties, including a linear delocalized  $\pi$  system, large conjugation length and extremely narrow HOMO–LUMO gap.<sup>1</sup> In view of these features, acenes are very valuable compounds as functional organic materials in optoelectronic applications.<sup>2</sup> Pentacene, for example, has been proven to be an efficient organic material for singlet fission and has been well employed in organic field-effect transistors (OFETs), organic photovoltaics (OPVs), and other organic electronic devices.<sup>3</sup> Longer acenes possess more attractive properties, like lower band gaps ( $\Delta E$ ) and better electronic properties than pentacene.<sup>4</sup> Unfortunately, the stability and solubility of acenes decrease notably along with the increase of length. All these inherent properties make the synthesis and functionalization of larger acenes a great challenge. Some

efforts have been made to synthesize and characterize hexacene since its first preparation reported by Clar in 1939.<sup>5</sup> In recent years, with great progress in scanning tunneling microscopy (STM) and other surface analysis techniques, on-surface synthesis provides a new method for the synthesis of acenes as well.<sup>6</sup> Krüger and co-workers reported on-surface generated hexacene by deoxygenation of the precursor triepoxyhexacene on Au(111) using STM in 2017.<sup>7</sup> The precursor triepoxyhexacene was synthesized in five steps. More recently, it was similarly generated using the same precursor on a H-passivated Si(001) surface.<sup>8</sup> The reported synthetic routes are depicted in Fig. 1, as a summary of the related literature. Among them, Watanabe and co-workers successfully obtained hexacene in a respectable quantity from a monoketone precursor that was synthesized in five steps.<sup>4a</sup>

Due to the enormous challenges in the synthesis of hexacene, the study of its electronic properties is inadequate. Only Watanabe and co-workers have reported its hole-transfer pro-

<sup>a</sup>School of Chemical Engineering, Nanjing University of Science and Technology, Nanjing 210094, China. E-mail: luojun@njust.edu.cn

<sup>b</sup>Herbert Gleiter Institute of Nanoscience, School of Materials Science and Engineering, Nanjing University of Science and Technology, Nanjing 210094, China. E-mail: konghuihui@njust.edu.cn

<sup>c</sup>Key Laboratory for Organic Electronics and Information Displays and Institute of Advanced Materials (IAM), Nanjing University of Posts and Telecommunications, Nanjing 210023, China. E-mail: iammdyi@njupt.edu.cn

†Electronic supplementary information (ESI) available: Synthetic details, NMR spectra, FT-IR spectra, X-ray crystal structure and data, and fabrication details of OFETs. CCDC 1887661. For ESI and crystallographic data in CIF or other electronic format see DOI: 10.1039/c9qo00708c

‡These authors contributed equally to this work.

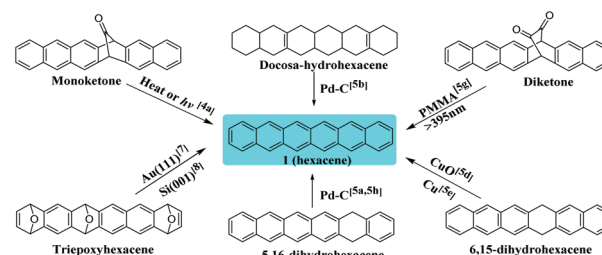
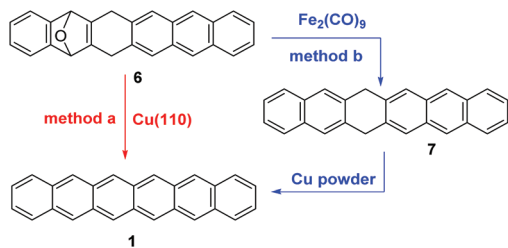


Fig. 1 Previously reported synthetic paradigms of hexacene.



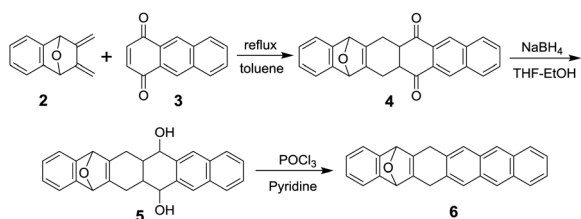
**Scheme 1** Generation of hexacene from: (a) precursor **6** by on-surface dehydration, and (b) dihydrohexacene precursor **7** by copper powder-catalyzed dehydrogenation.

erties; OFET devices made with single crystals of hexacene exhibited the highest hole mobility of  $4.28 \text{ cm}^2 \text{ V}^{-1} \text{ s}^{-1}$  and the OFET devices made with thin films of hexacene exhibited the highest hole mobility of  $7.6 \times 10^{-2} \text{ cm}^2 \text{ V}^{-1} \text{ s}^{-1}$ .<sup>4</sup> The best hole mobility of thin-film transistors is far from the best hole mobility of single-crystal transistors. Therefore, there is still a lot of research to be done for increasing the hole mobility of thin-film transistors. Developing an efficient method for the synthesis of hexacene is still in demand.

In this work, we reported a new and efficient synthetic route to synthesize hexacene *via* a new precursor (Scheme 1). Furthermore, we fabricated thin-film transistors by using hexacene through a vacuum deposition method and investigated their hole mobility.

## Results and discussion

Our work started with the construction of the backbone of hexacene. The air-stable precursor 5,6,15,16-tetrahydro-5,16-epoxyhexacene (**6**) was synthesized from commercially available materials by a three-step procedure in 31% total yield (Scheme 2). The synthesis commenced with 2,3-dimethylene-1,2,3,4-tetrahydro-1,4-epoxynaphthalene (**2**), which was prepared by the previously reported method.<sup>9</sup> The Diels–Alder reaction of compound **2** with 1,4-anthraquinone (**3**) afforded diketone derivative **4** in 51% yield. Compound **4** was reacted with  $\text{NaBH}_4$  to form the diol intermediate **5**. The effort to purify it by column chromatography failed at last. The reason might be attributed to its high sensitivity toward air. Then direct dehydration with  $\text{POCl}_3$  was performed and the key precursor **6** was obtained in a yield of 60% over two steps. The X-ray crystal structure of **6** is presented in Fig. S23.† It is stable under ambient conditions and soluble in  $\text{CH}_2\text{Cl}_2$ .



**Scheme 2** Synthesis of precursor **6**.

We expected that hexacene could be obtained by dehydration from precursor **6** by thermal activation on Cu(110) in an UHV environment at the single molecule level. Compared to the previous work on thermal-induced removal of a single H or O atom from precursors on the metal substrate, the simultaneous removal of two different atoms on different positions of certain precursors, as the two H atoms at 6 and 15 positions respectively and one O atom at 5 and 16 positions of molecule **6** in our experiment, has not been reported up to now.<sup>6–8</sup> This new method has the theoretical and practical significance for shortening the reaction steps and improving the synthesis efficiency. To verify our speculation, we prepared the sample in a preparation chamber and then transferred it to the STM chamber. The measurements were carried out at  $-196 \text{ }^\circ\text{C}$  with the aim of stabilizing the precursor molecules. Direct deposition of precursor **6** on Cu(110) held at room temperature (RT) resulted in the discrete distribution of precursor **6**, as shown by the blue ellipses in Fig. 2a (some impurities could also exist on the surface). The single-molecule length is around  $1.8 \pm 0.2 \text{ nm}$ , which is in good agreement with its theoretical length of 1.72 nm. Careful examination shows that precursor **6** was imaged as two parts with different apparent heights and the brighter part should be induced by the furan and methylene groups.

To investigate the on-surface reactions, we then performed heat treatment on the **6**-covered Cu(110) surface. Fig. 2b shows the STM topography after annealing at  $207 \text{ }^\circ\text{C}$ , which reveals that the molecular adsorption orientations have changed compared to Fig. 2a. Furthermore, the magnified STM image in

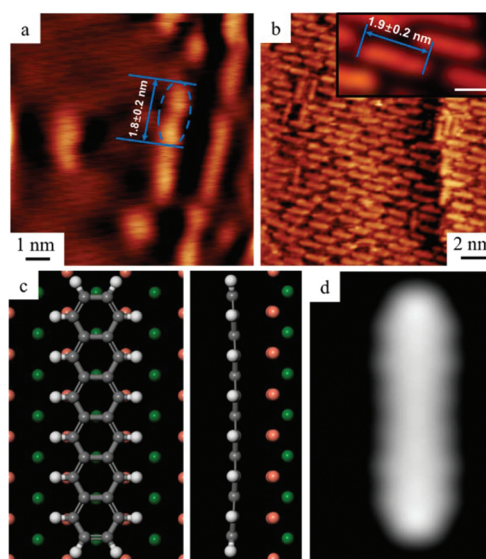


**Fig. 2** Thermal conversion of hexacene precursor **6** on the Cu(110) substrate. (a) STM image ( $V = 2 \text{ V}$ ,  $I = 50 \text{ pA}$ ) of precursor **6** deposited on Cu(110) at RT. (b) STM image ( $V = -1 \text{ V}$ ,  $I = 100 \text{ pA}$ ) showing the formation of hexacene by annealing at  $207 \text{ }^\circ\text{C}$ . The inset is a magnified STM image, revealing the details of hexacene. Scale bar: 1 nm. (c) Optimized geometry of hexacene on Cu(110) obtained by DFT calculations. Left: top view; right: side view. (d) STM simulation of hexacene on Cu(110).  $V = 1 \text{ V}$ .

the inset of Fig. 2b shows a uniform contrast of the molecule and the molecular length has changed to  $1.9 \pm 0.2$  nm (see the blue mark in Fig. 2b), which is in good agreement with the theoretical value of hexacene (1.80 nm). Besides, the simulated STM image (Fig. 2d) also shows a uniform contrast, which is consistent with that of hexacene (inset in Fig. 2b). These findings suggest that hexacene should be generated on Cu(110) by surface-assisted dehydration. Complementary insight into the adsorption geometry of hexacene on Cu(110) is obtained by DFT calculations. Fig. 2c shows the top and side view of the minimum-energy adsorption geometry, indicating that hexacene adopts a planar geometry on Cu(110), in agreement with the uniform contrast in the STM image, and that the long axis of hexacene is aligned with a high-symmetry direction of the substrate.

Although the above on-surface synthesis of hexacene proved its usefulness, a large-scale process is still of essential value for practical application. Based on the exciting results of STM experiments, we assumed that precursor **6** might also undergo dehydration to form hexacene in traditional chemical conversion in the solid state. To verify this, a mixture of **6** and an excess of copper powder was quickly heated to 270 °C and reacted for 1 h in an atmosphere of nitrogen. Unfortunately, though hexacene could be detected in the final reaction mixture by HPLC-MS analysis, the mixture was too complicated to isolate hexacene.

In order to obtain enough hexacene for practical application, we slightly adjusted the synthetic route. Deoxygenation of **6** by  $\text{Fe}_2(\text{CO})_9$  in toluene at 80 °C afforded 6,15-dihydrohexacene (**7**) in 65% yield (for synthetic details and characterization, see the ESI†). Compound **7** has been described in several articles.<sup>5a,d,e,h</sup> Then compound **7** was evenly mixed with copper powder. The mixture was quickly heated to 270 °C and reacted for 1 h in an atmosphere of nitrogen. The color of the reaction mixture gradually changed to blue-green. The pure target product hexacene was obtained by sublimation in the dark.

According to the FT-IR spectra, the characteristic methylene peak of dihydrohexacene at  $2925\text{ cm}^{-1}$  almost disappeared in the spectrum of hexacene (Fig. 3a). A 200-nm thick film of hexacene was successively prepared by thermal evaporation (base pressure:  $5.0 \times 10^{-6}$  Pa) with a deposition rate of  $1\text{ \AA s}^{-1}$  and the quartz substrate temperature was maintained at room temperature. The green film showed UV/Vis absorption at 834 nm, 767 nm, 703 nm and 660 nm, which is in accordance with the reported data of hexacene (Fig. 3b). The spectrum of high-resolution atmospheric pressure chemical ionization mass spectroscopy (HR-APCI-MS) exhibited a molecular ion signal at  $m/z$  329.1304 (Fig. 3c), which is in accordance with hexacene ( $\text{MH}^+$ , calcd 329.1330). Due to its sensitivity to air and light, hexacene was oxidized during the sample preparation process. A significant signal at  $m/z$  359 can be seen in Fig. 3c. The solid-state cross-polarization magic angle spinning (CP-MAS) NMR spectrum of hexacene showed only aromatic absorption bands at 120–135 ppm (Fig. 3d).

To study the charge transport characteristics of hexacene, we fabricated bottom-gate, top-contact OFETs by employing

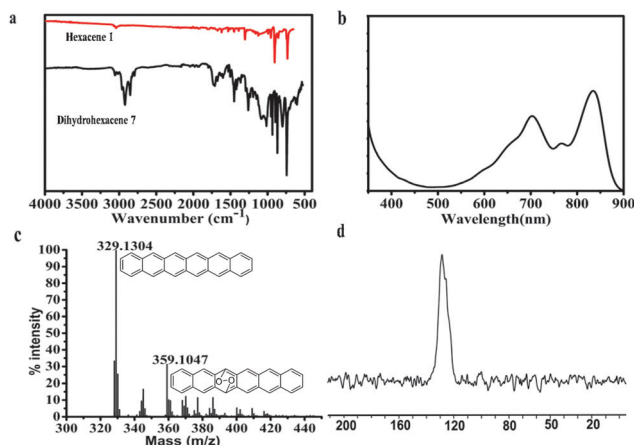


**Fig. 3** Characterization of hexacene: (a) infrared spectra of precursor **7** (bottom) and hexacene (top); (b) absorption spectra of a thin film of hexacene measured in the dark under ambient conditions; (c) HR-APCI-MS chart of hexacene; and (d)  $^{13}\text{C}$  CP/MAS NMR spectrum of hexacene.

hexacene as the semiconducting channel. These devices were prepared on heavily doped n-type Si wafer with a  $\text{SiO}_2$  layer (50 nm), serving as the gate electrode and gate insulator layer, respectively. Surface modification of the gate dielectric using polymers and self-assembly monolayers (SAMs) prior to the deposition of an organic semiconductor layer is a general approach for improving the charge transport properties of OFETs.<sup>10</sup> Here, the  $\text{SiO}_2$  surface was modified with insulating polymers, including polystyrene (PS), poly(methyl methacrylate) (PMMA) and SAMs of octadecyltrichlorosilane (OTS), respectively. Subsequently, 50-nm thick hexacene was grown through a vacuum deposition method. Finally, 50-nm thick source and drain electrodes were deposited by thermal evaporation of Au through the metal shadow mask. The atomic force microscopy (AFM) images of the films of hexacene are shown in Fig. S5 (ESI†), showing that the PS-modified film has a lower roughness. The electrical measurements were carried out under air in the dark. Fig. 4 shows the output and transfer characteristics of a PS-modified OFET, where representative p-type field-effect transistor behavior was observed. Table 1 summarizes the electrical parameters for OFETs with different modifications. All the parameters were extracted from transfer curves that were measured from at least 30 channels on 6 inde-

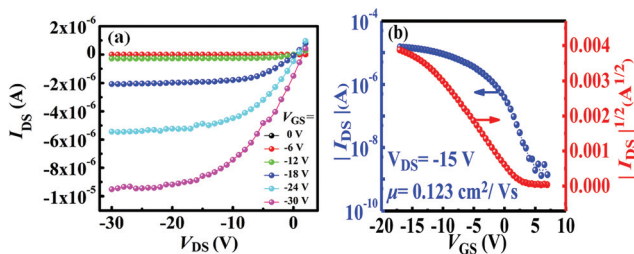


**Fig. 4** Thin-film OFETs made using hexacene with a polystyrene dielectric layer. (a) Output characteristics; (b) transfer characteristics.

**Table 1** Performance of hexacene as measured from thin-film transistors

SiO <sub>2</sub>	Dielectric layer	$\mu$ (cm <sup>2</sup> V <sup>-1</sup> s <sup>-1</sup> )	$I_{on}/I_{off}$	$V_{th}$ (V)
50 nm	PS	0.103	$1.89 \times 10^4$	3.47
	PMMA	0.050	$5.24 \times 10^4$	-4.43
	OTS	0.059	$6.86 \times 10^4$	-10.52

pendent substrates for each kind of OFET device. The average hole mobilities of hexacene-based OFETs are in the range of 0.050–0.103 cm<sup>2</sup> V<sup>-1</sup> s<sup>-1</sup> and a threshold of -10.52–3.47 V. Noticeably, a PS-modified OFET exhibits the highest hole mobility of 0.123 cm<sup>2</sup> V<sup>-1</sup> s<sup>-1</sup> with an on/off ratio of  $1.16 \times 10^4$  and a threshold of 2.65 V (Fig. 4), which is also the highest value in the previously reported mobilities for hexacene-based OFETs to the best of our knowledge. These results show that hexacene has the potential to be used as a semiconducting material for the fabrication of high-mobility OFETs. At the same time, the research shows that the mobility of organic field-effect transistors could be effectively improved *via* ameliorating the surface properties of the dielectric.

## Conclusions

In summary, 5,6,15,16-tetrahydro-5,16-epoxyhexacene was first synthesized through an efficient route. Hexacene molecules could be generated on the Cu(110) surface by dehydration of the precursor under UHV conditions according to STM imaging. Although hexacene could also be formed by copper powder-catalyzed dehydration of this precursor, the reaction mixture is too complicated to isolate hexacene. We slightly adjusted the synthetic route and successfully obtained pure hexacene by powder-catalyzed dehydrogenation of 6,15-dihydrohexacene, which is prepared from 5,6,15,16-tetrahydro-5,16-epoxyhexacene by deoxygenation catalyzed by Fe<sub>2</sub>(CO)<sub>9</sub>. This is a new and efficient synthesis method. Organic thin-film transistors were fabricated by using hexacene through a vacuum deposition method. The fabrication conditions were optimized, and the hole mobility was promoted to 0.123 cm<sup>2</sup> V<sup>-1</sup> s<sup>-1</sup>, which is the highest value for thin-film transistors based on hexacene to the best of our knowledge.

## Conflicts of interest

There are no conflicts to declare.

## Acknowledgements

This work was sponsored by the National Natural Science Foundation of China (21802072 and 61775100) and the Qing Lan Project of Jiangsu Province (2014), P. R. China. The authors are grateful to Dr Yue Zhao and Dr Hongjuan Chen

from Nanjing University for the single-crystal structure analysis and mass spectra analysis, respectively.

## Notes and references

- (a) M. Bendikov, F. Wudl and D. F. Perepichka, *Chem. Rev.*, 2004, **104**, 4891–4945; (b) H. F. Bettinger and C. Tönshoff, *Chem. Rec.*, 2015, **15**, 364–369; (c) J. E. Anthony, *Chem. Rev.*, 2006, **106**, 5028–5048; (d) J. Roncali, P. Leriche and P. Blanchard, *Adv. Mater.*, 2014, **26**, 3821–3838; (e) M. Watanabe, K. Chen, Y. J. Chang and T. J. Chow, *Acc. Chem. Res.*, 2013, **46**, 1606–1615; (f) T. J. Chow, *Chem. Rec.*, 2015, **15**, 1137–1139.
- (a) Q. Ye and C. Chi, *Chem. Mater.*, 2014, **26**, 4046–4056; (b) D. Xiang, X. Wang, C. Jia, T. Lee and X. Guo, *Chem. Rev.*, 2016, **116**, 4318–4440; (c) H. I. Un, P. Cheng, T. Lei, C. Y. Yang, J. Y. Wang and J. Pei, *Adv. Mater.*, 2018, **30**, 1800017; (d) O. Ostroverkhova, *Chem. Rev.*, 2016, **116**, 13279–13412; (e) A. Naibi Lakshminarayana, A. Ong and C. Chi, *J. Mater. Chem. C*, 2018, **6**, 3551–3563; (f) N. Monahan, D. Sun, H. Tamura, K. Williams, B. Xu, Y. Zhong, B. Kumar, C. Nuckolls, A. Harutyunyan, G. Chen, H. Dai, D. Beljonne, Y. Rao and X. Zhu, *Nat. Chem.*, 2017, **9**, 341–346; (g) C. K. Yong, A. J. Musser, S. L. Bayliss, S. Lukman, H. Tamura, O. Bubnova, R. K. Hallani, A. Meneau, R. Resel, M. Maruyama, S. Hotta, L. M. Herz, D. Beljonne, J. E. Anthony, J. Clark and H. Sirringhaus, *Nat. Commun.*, 2017, **8**, 15953.
- (a) W. Li, F. Guo, H. Ling, P. Zhang, M. Yi, L. Wang, D. Wu, L. Xie and W. Huang, *Small*, 2018, **14**, 1701437; (b) S. H. Yuan, Z. Pei, H. C. Lai, P. W. Li and Y. J. Chan, *Org. Electron.*, 2015, **27**, 7–11; (c) K. Broch, J. Dieterle, F. Branchi, N. J. Hestand, Y. Olivier, H. Tamura, C. Cruz, V. M. Nichols, A. Hinderhofer, D. Beljonne, F. C. Spano, G. Cerullo, C. J. Bardeen and F. Schreiber, *Nat. Commun.*, 2018, **9**, 954; (d) B. S. Basel, J. Zirzmeier, C. Hetzer, B. T. Phelan, M. D. Krzyaniak, S. R. Reddy, P. B. Coto, N. E. Horwitz, R. M. Young, F. J. White, F. Hampel, T. Clark, M. Thoss, R. R. Tykwinski, M. R. Wasielewski and D. M. Guldi, *Nat. Commun.*, 2017, **8**, 1571.
- (a) M. Watanabe, Y. J. Chang, S. W. Liu, T. H. Chao, K. Goto, M. M. Islam, C. H. Yuan, Y. T. Tao, T. Shinmyozu and T. J. Chow, *Nat. Chem.*, 2012, **4**, 574–578; (b) M. Watanabe, T. Miyazaki, T. Matsushima, J. Matsuda, C. Chein, M. Shibahara, C. Adachi, S. Sun, T. Chow and T. Ishihara, *RSC Adv.*, 2018, **8**, 13259–13265.
- (a) E. Clar, *Ber. Dtsch. Chem. Ges B*, 1939, **72**, 1817–1821; (b) W. J. Bailey and C. W. Liao, *J. Am. Chem. Soc.*, 1955, **77**, 992–993; (c) P. Grüninger, M. Polek, M. Ivanović, D. Balle, R. Karstens, P. Nagel, M. Merz, S. Schuppler, R. Ovsyannikov, H. F. Bettinger, H. Peisert and T. Chassé, *J. Phys. Chem. C*, 2018, **122**, 19491–19498; (d) E. Clar, *Ber. Dtsch. Chem. Ges B*, 1942, **75**, 1283–1285; (e) M. P. Satchell and B. E. Stacey, *J. Chem. Soc. C*, 1971, 468–469;

- (f) R. Mondal, R. M. Adhikari, B. K. Shah and D. C. Neckers, *Org. Lett.*, 2007, **9**, 2505–2508; (g) R. Mondal, B. K. Shah and D. C. Neckers, *J. Am. Chem. Soc.*, 2006, **128**, 9612–9613; (h) S. Toyota and T. Iwanaga, *Sci. Synth.*, 2010, **45b**, 745–854.
- 6 (a) J. Krüger, N. Pavliček, J. M. Alonso, D. Pérez, E. Guitián, T. Lehmann, G. Cuniberti, A. Gourdon, G. Meyer, L. Gross, F. Moresco and D. Peña, *ACS Nano*, 2016, **10**, 4538–4542; (b) H. Kong, S. Yang, H. Gao, A. Timmer, J. P. Hill, O. Diaz Arado, H. Monig, X. Huang, Q. Tang, Q. Ji, W. Liu and H. Fuchs, *J. Am. Chem. Soc.*, 2017, **139**, 3669–3675; (c) R. Zuzak, R. Dorel, M. Kolmer, M. Szymonski, S. Godlewski and A. M. Echavarren, *Angew. Chem., Int. Ed.*, 2018, **57**, 10500–10505.
- 7 J. Krüger, F. Eisenhut, J. M. Alonso, T. Lehmann, E. Guitián, D. Pérez, D. Skidin, F. Gamaleja, D. A. Ryndyk, C. Joachim, D. Peña, F. Moresco and G. Cuniberti, *Chem. Commun.*, 2017, **53**, 1583–1586.
- 8 F. Eisenhut, J. Krüger, D. Skidin, S. Nikipar, J. M. Alonso, E. Guitián, D. Pérez, D. A. Ryndyk, D. Peña, F. Moresco and G. Cuniberti, *Nanoscale*, 2018, **10**, 12582–12587.
- 9 J. Luo and H. Hart, *J. Org. Chem.*, 1989, **54**, 1762–1764.
- 10 C. Di, Y. Liu, G. Yu and D. Zhu, *Acc. Chem. Res.*, 2009, **42**, 1573–1583.